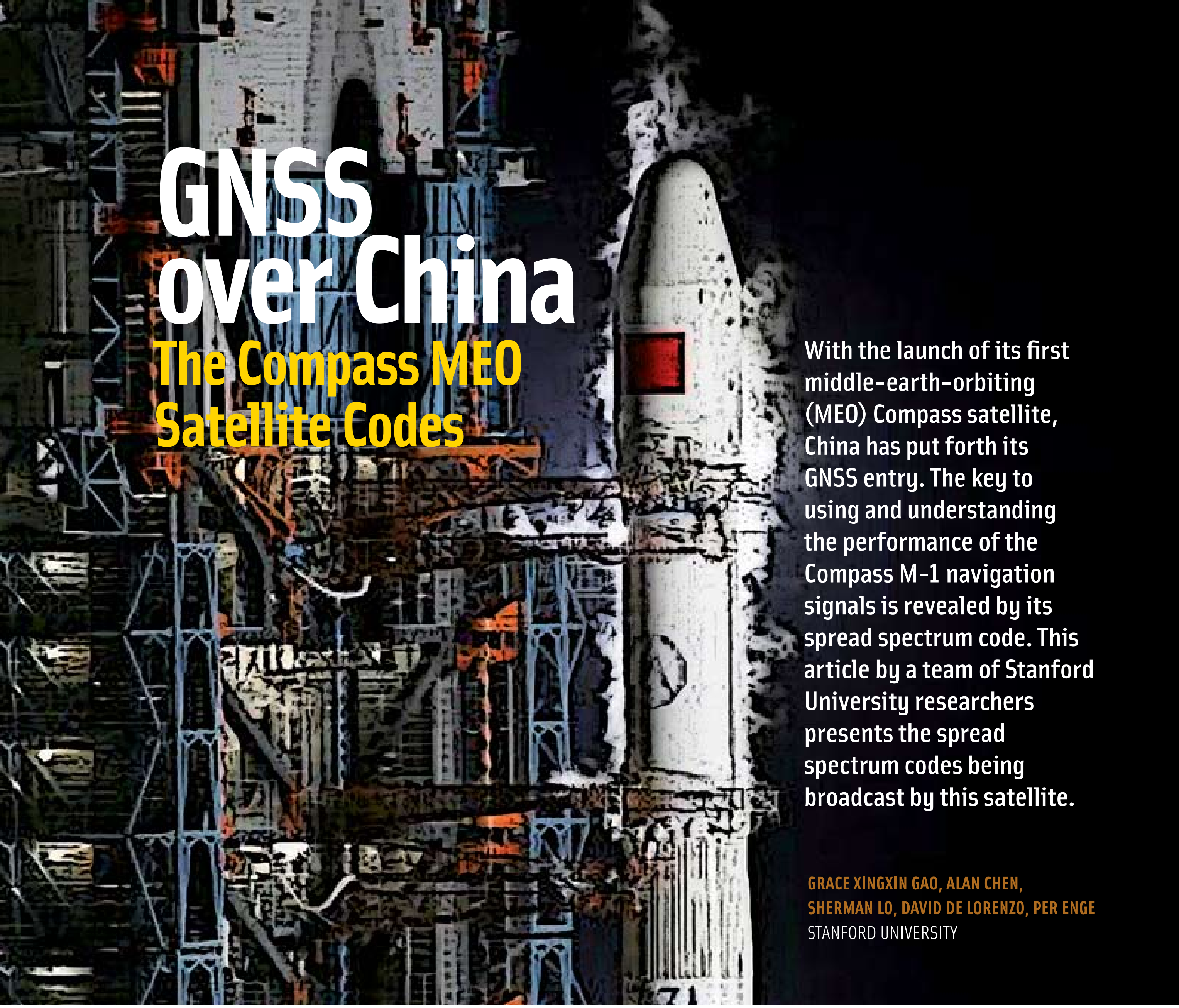

GNSS over China

The Compass MEO Satellite Codes

With the launch of its first middle-earth-orbiting (MEO) Compass satellite, China has put forth its GNSS entry. The key to using and understanding the performance of the Compass M-1 navigation signals is revealed by its spread spectrum code. This article by a team of Stanford University researchers presents the spread spectrum codes being broadcast by this satellite.

GRACE XINGXIN GAO, ALAN CHEN, SHERMAN LO, DAVID DE LORENZO, PER ENGE
STANFORD UNIVERSITY

On April 14, 2007 (local time), China launched the Compass M-1 satellite. This satellite represents the first of a new global navigation satellite system (GNSS) that is planned to have a total of 35 satellites. Unlike prior Chinese navigation satellites, Compass M-1 broadcasts in L-band, using signal structures similar to other GNSS systems and sharing frequencies near to or overlapping those of GPS, Galileo, and GLONASS.

The addition of another GNSS, particularly one that will broadcast in the same frequency bands as GPS and Galileo, both excites and intrigues the GNSS community. Such a system has the potential to introduce benefits — as well as concerns — for GNSS users. Numerous researchers around the world, including Stanford University (SU), have been interested in examining the navigation signal of this system.

To understand its effects and to develop receivers that can track the signal, one must understand the signal structure being used. In the case of Compass, this means determining and understanding its spread spectrum codes. This article will present the Compass codes and provide an overview of how our team at Stanford determined these.

Compass Overview

The Beidou (北斗) or Compass navigation satellite system (CNSS) is China's entry into the realm of GNSS. The current design is have a system comprised of 30 medium earth orbit (MEO) satellites and 5 geostationary orbit (GEO) satellites. The MEO satellites will operate in six orbital planes to provide global navigation coverage.

Compass will share many features in common with GPS and Galileo, providing the potential for low cost integration of these signals into a GPS/Galileo/Compass receiver. These commonalities include multiple frequencies, signal structure, and services.

According to International Telecommunication Union (ITU) filings by China, Compass will broadcast on four frequencies centered at 1590 MHz, 1561 MHz, 1269 MHz, and 1207 MHz (rounded). **Table 1** provides general information on the signals in each of these frequencies. These signals, then, lie in the frequency band of GPS and Galileo signals.

The Compass navigation signals are code division multiple access (CDMA) signals similar to the GPS and Galileo signals. They use binary or quadrature phase shift keying (BPSK, QPSK, respectively). Further, SU observations and analysis indicate that the codes from the current Compass M-1 are derived from Gold codes.

Statements from Chinese sources indicate that the system will provide at least two services: an open civilian service and a higher precision military/authorized user service.

The Compass-M1 satellite represents the first of this next generation of Chinese navigation satellites and differs significantly from China's previous Beidou navigation satellites. Those earlier satellites were considered experimental, and most were developed for two-dimensional positioning using the radio determination satellite service (RDSS) concept pioneered by Geostar.

Compass M-1 is also China's first MEO navigation satellite. Previous Beidou satellites were geostationary and only provide coverage over China. The *global* implications of this satellite and the new GNSS it represents makes the satellite of great interest to navigation experts.

The rapid manner in which researchers have already trained their instruments onto the satellite proves this point. For example, Centre National d'Études Spatiales (CNES, the French space agency) published an informative overview of their observations of the Compass-M1 signals a month after its launch in the May/June issue of *Inside GNSS*.

The interest has resulted in significant basic information on the Compass M-1 satellite. Observations by CNES, SU, and other researchers indicate that the current satellite is only broadcasting on three of the frequencies (E2, E6, E5b).

Frequency	Modulation Type
1589.74 (E1)	QPSK(2)
1561.1 (E2)	QPSK(2)
1268.52 (E6)	Q/BPSK(10)
1207.14 (E5b)	BPSK(2), BPSK(10)

TABLE 1. Compass Frequencies and Modulation

To the best of the authors' knowledge, no observations of Compass E1 broadcasts have been made. It also appears that the Compass satellite is not continuously broadcasting navigation messages on the other three frequencies; we have occasionally observed unmodulated or continuous wave (CW) signals in those bands. Apart from these basic observations of the Compass M-1 signal structure, little information has been published on the actual codes.

The similarity in frequency, signal structure, and services with GPS and Galileo makes Compass a tantalizing prospect for GNSS users. These similarities could allow for the addition of Compass to an integrated GNSS receiver without additional expensive hardware or processing. Moreover, the rapid progress of the Compass development (and the current state of the Galileo program) offers the intriguing possibility that the system may become operational before Galileo.

As such, great motivation exists for understanding Compass and how it may be properly and cost-effectively integrated into a GNSS receiver. On the flip side, the signals may pose a source of interference and degrade the performance of GPS or Galileo. Interference with and degradation of GPS/Galileo performance are possibilities if interoperability was not a driving concern in the signal design.

This latter possibility, of course, concerns military users as well because Compass overlays the GPS M-code and

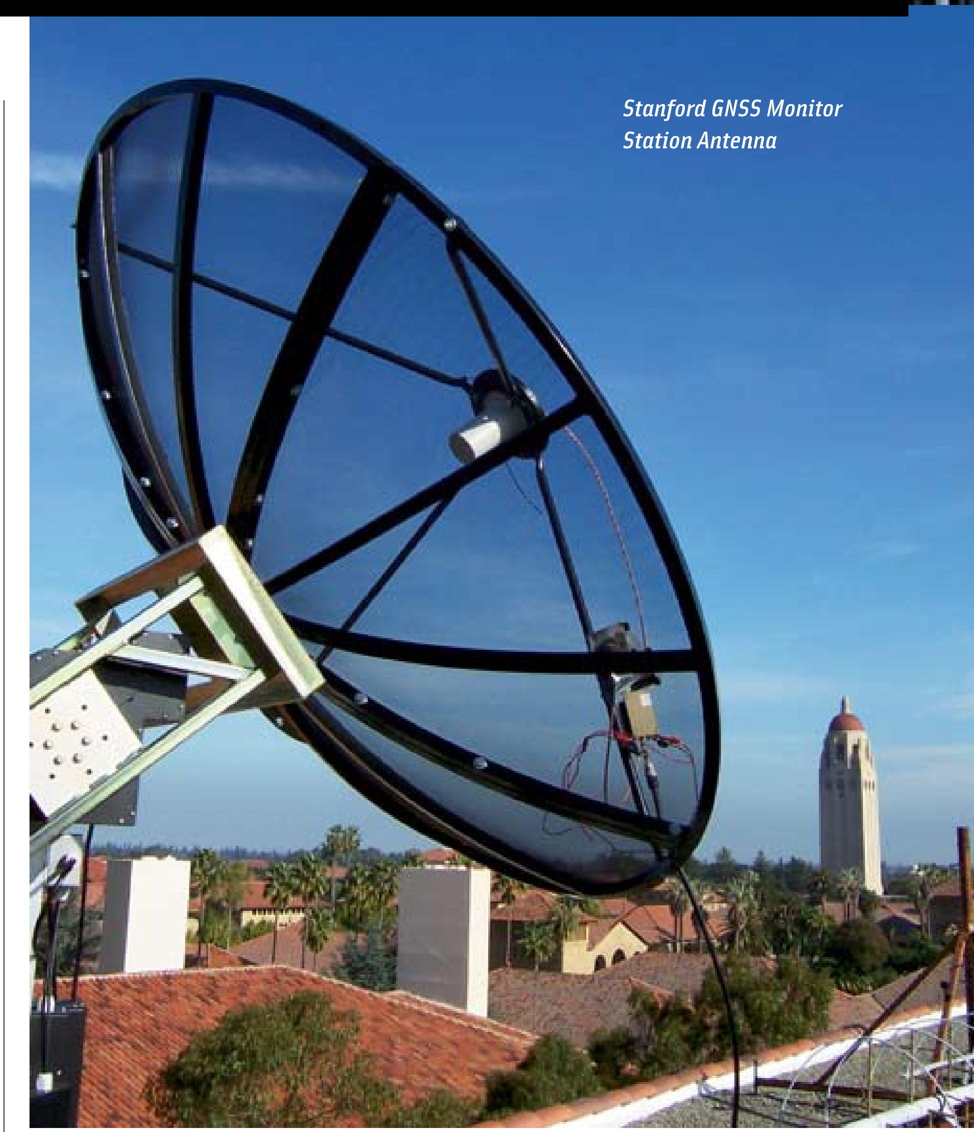

Stanford GNSS Monitor Station Antenna

Portable Ground Station Set Up

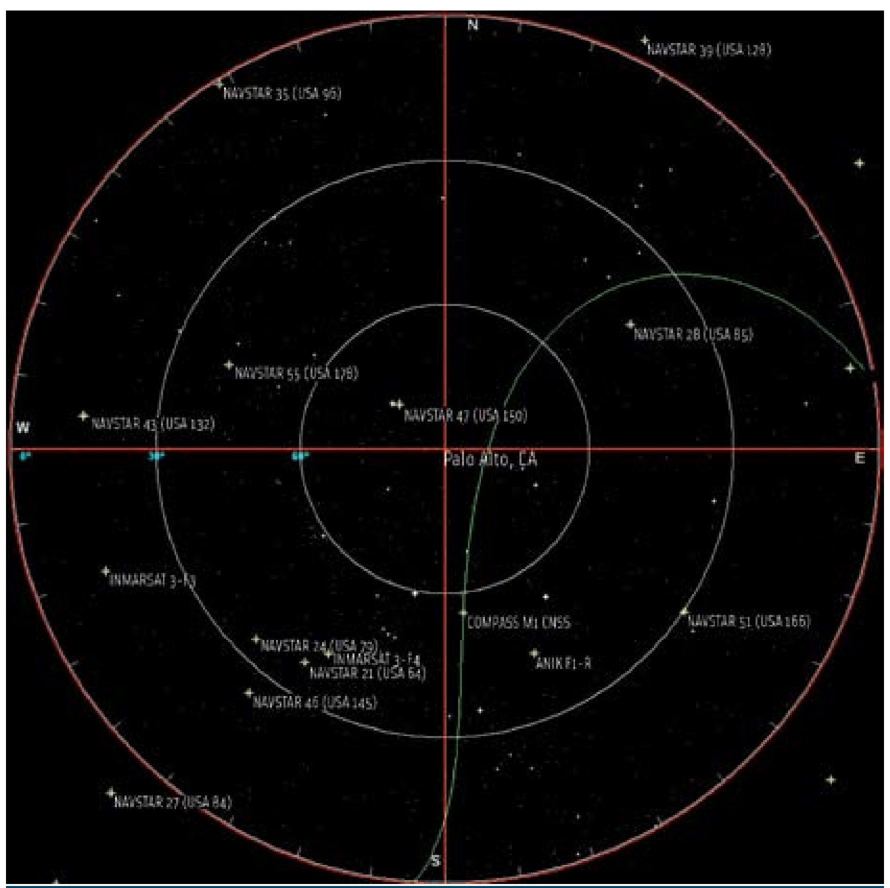

FIGURE 1 Sky plot of Compass satellite visible over Palo Alto, California (Stanford University) on May 7, 2007

Galileo public regulated service (PRS) on E1/E2. Hence, understanding the signal design and modulation is important in order to determine the Compass system's potential for interoperability and interference.

The first step toward this latter goal is to determine the Compass codes. This will help to develop prototype GPS/Galileo/Compass receivers and help identify ways to best use the new signals together with other planned or existing GNSS signals.

Data Collection Equipment

Use of a high gain antenna greatly aids the effort to assess the Compass signal and determine its navigation code. For data collection, we used the Stanford GNSS Monitor Station (SGMS). The SGMS has a 1.8-meter steerable parabolic dish antenna with an L-band feed. The system was developed to provide an on-demand capability for observing GNSS signals.

This antenna provided many of the measurements seen in a previous article in the May/June 2006 issue of *Inside GNSS* to which the authors contributed, including some of the data used to determine and validate the GIOVE-A codes. (See the citation for the article by S. Lo et alia in the "Additional Resources" section near the end of the article.)

We collected data for the analysis described here using a vector signal analyzer (VSA). One change from our past set-up was to make the ground station (including antenna controllers) portable. This was necessary because the original ground station facility is being renovated. Accompanying photos show the SU antenna and ground station.

Data sets on all three observed Compass frequencies were taken on multiple days. The first data sets were logged on May 7, 2007. We verified the signal in each frequency band using spectrum plots from the VSA. As the SGMS provides approximately 25 decibels (dB) of gain above that of a standard patch antenna, the main lobe of the Compass signals were clearly visible.

Additionally, the Compass satellite was generally at high elevation when the observations were made. The sky plot of the GNSS satellites visible on this date is seen in **Figure 1**.

Analysis of the short data sets from May 7 indicated that the Compass E2 quadrature channel (Q-channel) had a significantly longer sequence than the in phase channel (I-channel). As a result, we collected additional data in June in order to obtain longer data sets with which to work.

Frequency Domain Plots

Rather than repeat the excellent spectrum plots from the CNES article mentioned earlier, this section will show the spectrum for each Compass signal without averaging. **Figure 2** shows the unaveraged E2 signal spectrum from one of our data sets. The main lobe and the first side lobes of the 2 MHz chipped signal are clearly visible even without averaging.

An L1 signal from a nearby GPS satellite can also be seen in this plot as well as narrowband signals on 1549 MHz. **Figure 3** shows the unaveraged Compass E5b signal spectrum from another data set. The main lobe of the BPSK(2) is clearly visible, and the BPSK(10) main lobe can also be made out. As expected in this frequency band, we also see strong narrowband interference from distance measuring equipment (DME).

Figure 4 shows the unaveraged E6 signal spectrum with the main feature being the main lobe of the QPSK(10) signal. Also visible is an as yet unidentified 1 MHz–wide transmission centered around 1257 MHz.

Deriving the Compass Codes

The main challenge to revealing the PRN code sequence is the low signal-to-noise ratio (SNR). With an omnidirectional antenna, the received signal power is on the order of 10^{-16} watts. Even with the 1.8-meter dish antenna and high-quality low noise amplifiers (LNA), the received C/No is still roughly 65-70 dB-Hz (assuming a transmit power of 30 W). This still does not provide enough gain to pull the code chips out of the noise, and the code is not directly visible in the time domain.

In order to decode the PRN code sequence, we need to process the data to boost the signal above the noise floor. The main concept is to stack multiple periods of the PRN sequence together so that the noise will be averaged. To achieve this, we need to determine the code period, wipe off Doppler offset, adjust the initial phase shift and demodulate the secondary code.

The following section provides an overview of the process we applied, using the Compass E2 I-channel code as the example. We employed a similar methodology in the other frequency bands.

Code Sequence Demodulation. We determined the code period by correlating the signal with a slice of itself, as shown in **Figure 5**. The inter-peak interval reveals the primary code period to be one millisecond. The height of the peaks varies due to the Doppler offset, which results in constant phase variation. The variation creates peaks in the I and Q channels, modulating the real and imaginary parts with a cosine and sine wave, respectively.

In order to remove the Doppler offset, we search the whole Doppler domain from -10,000 Hz to 10,000 Hz and minimize the peak height variation after Doppler compensation. After wiping off the Doppler, we can see peaks with more uniform heights in the in-phase channel and no peak in the quadrature

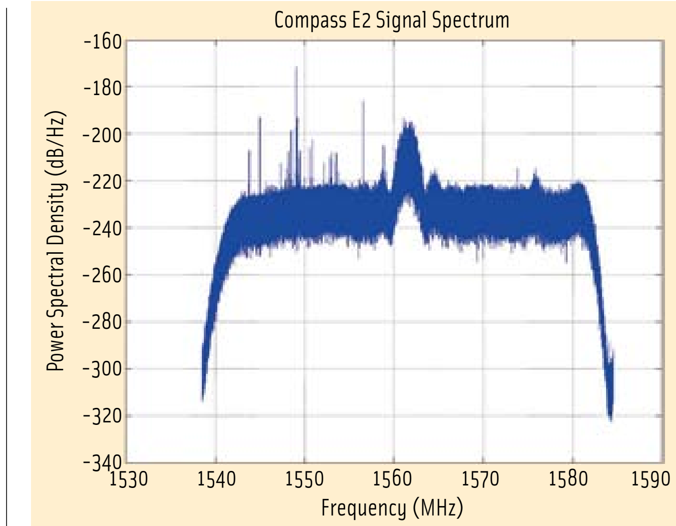

FIGURE 2 Unaveraged spectrum of Compass M-1 E2

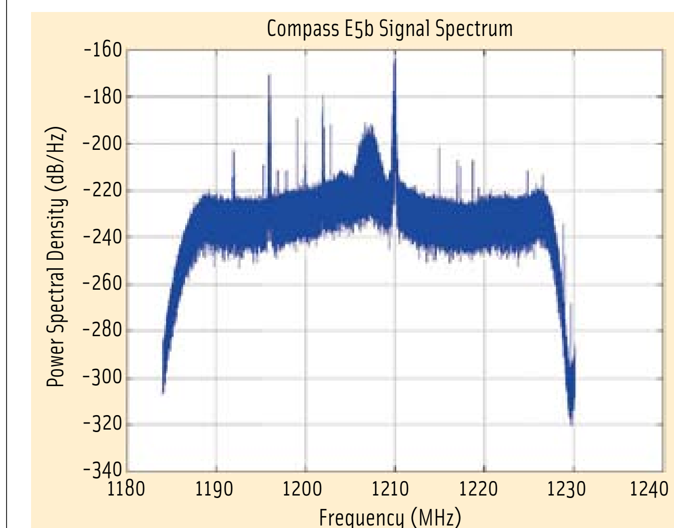

FIGURE 3 Unaveraged spectrum of Compass M-1 E5b

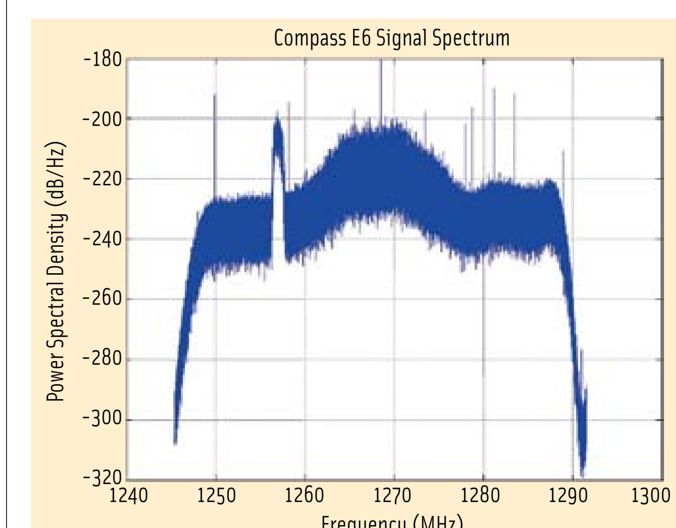

FIGURE 4 Unaveraged Spectrum of Compass M-1 E6

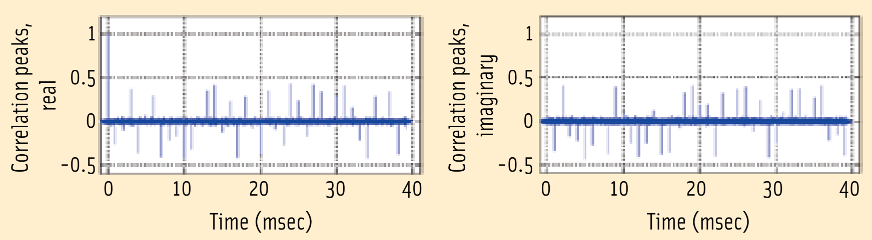

FIGURE 5 Correlation of the Compass E2 signal with a slice of itself

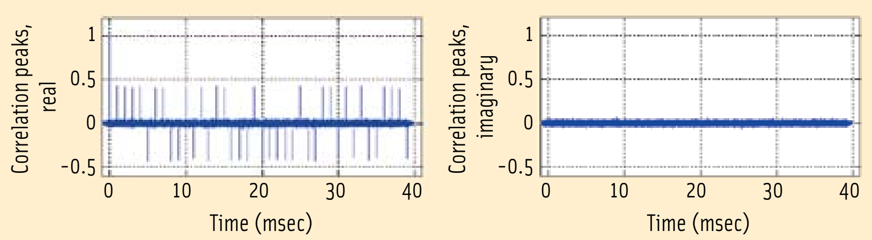

FIGURE 6 Correlation of the Compass E2 signal with a slice of itself, after Doppler wipeoff

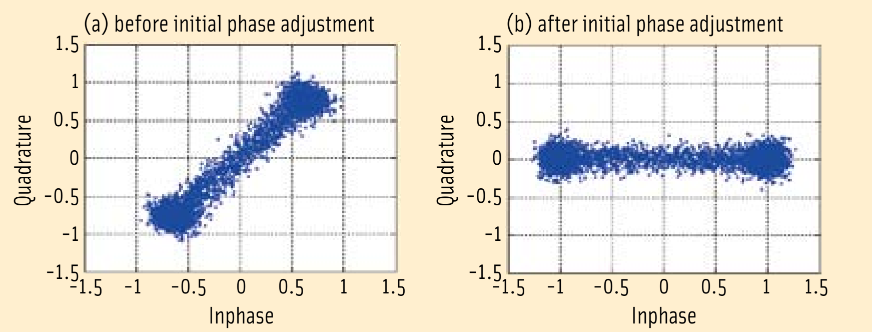

FIGURE 7 Compass E2 signal I-channel time-domain scatter plot

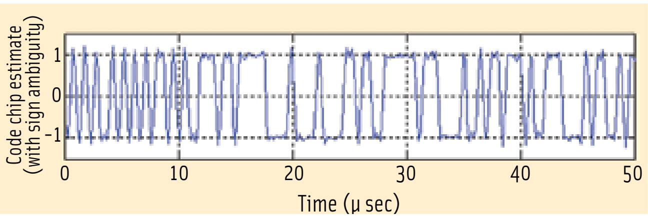

FIGURE 8 First 50 microseconds of the Compass E2 I-channel PRN code

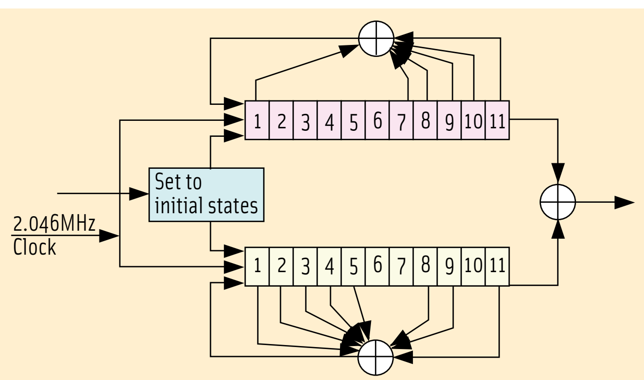

FIGURE 9 Code generator schematic of the Compass E2 I-channel signal

channel as shown in Figure 6. This verifies the correctness of our Doppler offset estimate.

Wiping off the Doppler reveals the data on top of the E2 I-channel, as seen in Figure 6. In this case, the data is the E2 I-channel secondary code. The secondary code is just the polarity/sign imposed on each period of the primary E2 I-channel PRN code.

We then use this information to wipe off the secondary code, so that every period of the primary code has the same polarity. Next, we stack multiple periods of the code together to increase the code energy and average down the noise.

The initial phase shift is then adjusted so that the center axis of the points in the time-domain scatter plot is aligned with the in-phase axis, as shown in Figure 7.

After these steps, we decoded the E2 I-channel PRN code sequence. Figure 8 shows the first 50 microseconds of the code. After down sampling, the code bits are obtained. The E2 I-channel PRN code is 2,046 bits long and lasts for one millisecond.

Note that the sign of the secondary code is ambiguous, as the sign of the first bit of the secondary code is not determined yet. This may cause the sign of the PRN code sequence to flip. The sign ambiguity problem can be solved once we derive the code generator.

Deriving Code Generators. With the code sequence obtained, we can implement these PRN sequences in a software receiver for acquisition and tracking. However, we would also like to study the code structure, which will help us understand the effects of this code on other signals in the frequency band.

Furthermore, determining the PRN code generators will help minimize the code representation if the code is derived from linear codes. The last point is particularly important, because storing thousands of bits in the receiver is expensive in terms of flash memory and even more expensive in digital signal processing (DSP) units.

Our analysis has proven that the code is linear and can be generated by a 22nd-order linear shift feedback registers (LSFR). (The two papers by G. Gao *et alia* cited in the Additional Resources section present the procedures of the proof.) The 22nd-order LSFR polynomials can be further factorized into two 11th-order polynomials. This indicates that the Compass E2 I-channel PRN code is an 11-stage Gold code.

The code generator polynomials and initial states are shown in Table 2. The PRN code generator schematic is shown in Figure 9.

The sign ambiguity can be solved after deriving the PRN code polynomials. If the PRN code polynomial can be factorized by "1+X," then the code is flipped. Otherwise, it is not. This is because the polynomial "1+X" generates a sequence of all "1s." When it is added modulo 2 to the code sequence, all the resultant code bits flip signs.

Now we have solved the sign ambiguity for the secondary code sequence. The secondary code turns out to be a Neuman Hoffman code with the following sequence:: -1 -1 -1 -1 -1 1 -1 -1 1 1 -1 1 -1 1 -1 -1 1 1 1 1 -1

Acquisition and Tracking

With the decoded codes, signals from the Compass M-1 satellite can be acquired and tracked with a multi-signal all-in-view GNSS software receiver implemented in MATLAB. SU developed this receiver based on the integration of our own receiver code and receiver code from the University of Aalborg, Denmark, and Prof. Dennis Akos of the University of Colorado, Boulder. We loaded raw Compass data collected at 4 MHz signal bandwidth (5.12 MHz sample rate) using the SGMS into the software receiver to test the efficacy of the derived codes.

Acquisition is implemented as a parallel code-phase search using FFT-based processing. Several milliseconds of data may be combined to increase weak-signal sensitivity or to provide more accurate estimates of carrier Doppler frequency, although at a trade-off in execution time.

The 3-D acquisition plot in Figure 10 shows the normalized correlation function output as a function of code phase on one axis and carrier Doppler frequency on the other axis. A small amount of averaging (two milliseconds) was used. We read the code phase and Doppler estimate based on the location of the main peak in the code phase and Doppler domain.

Immediately after acquisition, the code phase and carrier frequency estimates are used to initialize the code and carrier numerically-controlled oscillators (NCOs). The receiver refines the estimates of carrier frequency, carrier phase, and code phase through a succession of tracking modes. This step successively reduces the phase-lock and delay-lock loop (PLL and DLL, respectively) noise bandwidths.

The tracking output in Figure 11 shows four subplots as follows, each as a function of elapsed tracking time along the horizontal axis:

- upper-left: PLL discriminator output in degrees
- upper-right: DLL discriminator output in meters (150 m = 1 chip)
- lower-left: carrier Doppler frequency estimate
- lower-right: code-phase estimate with respect to the receiver's on-board millisecond counter

Because one of our tracking objectives was the estimation of the secondary code length and sequence, we kept integration times to one millisecond for all tracking modes (the length of the primary spreading code sequence). We did this because carrier polarity may change at each millisecond, and this sequence is unknown until the secondary decoding has occurred.

All tracking outputs converge, such as phase offset, code offset, and Doppler frequency. The PLL converges quickly. However, the DLL discriminators take a bit longer to settle to roughly zero offset.

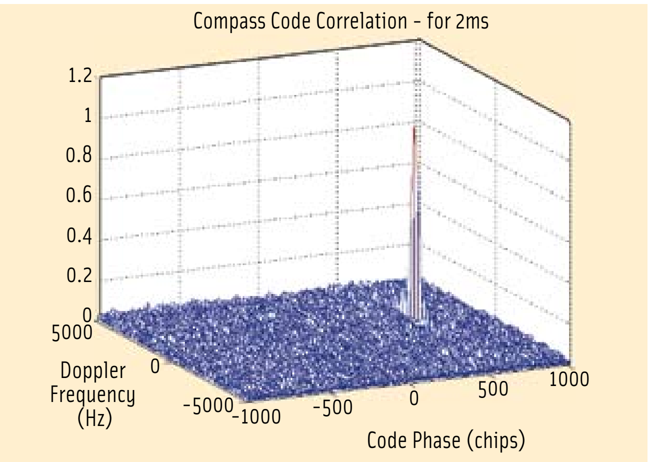

FIGURE 10 Acquisition plot of Compass M-1 E2 I-channel

E2 I-channel code (2046 bits, 1msec, 11-stage Gold code)	
Polynomial_1	$X^{11}+X^{10}+X^9+X^8+X^7+X+1$
Initial State_1	[0 1 0 1 0 1 0 1 0 1 0]
Polynomial_2	$X^{11}+X^9+X^8+X^5+X^4+X^3+X^2+X+1$
Initial State_2	[0 0 0 0 0 0 0 1 1 1 1]

TABLE 2. Code generator polynomials and initial states of the Compass E2 I-channel signal

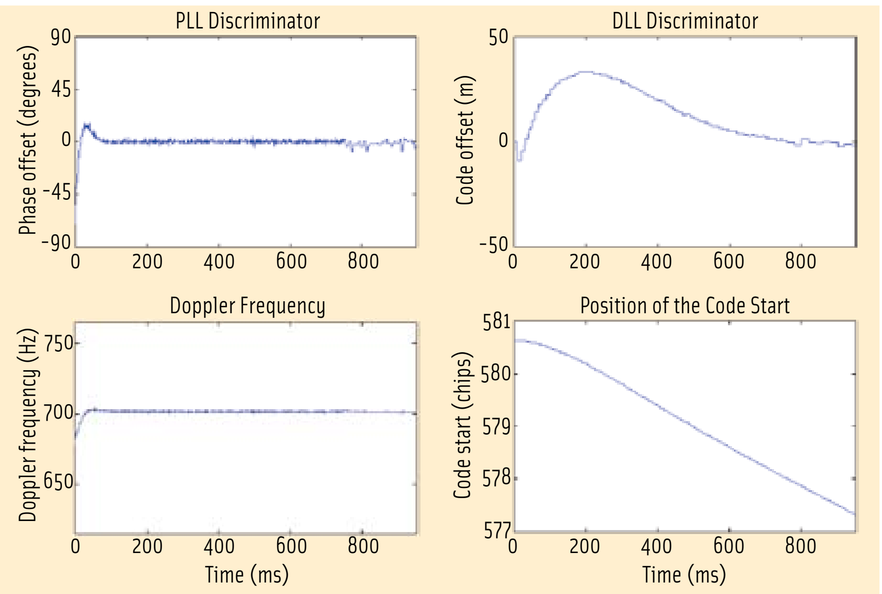

FIGURE 11 Tracking results of Compass M-1 E2 I-channel

E6 I-channel code (Head)	
Polynomial_1	$X^{13}+X^{12}+X^{10}+X^{9}+X^{7}+X^{6}+X^{5}+X+1$
Initial State_1	[1 1 1 1 1 1 1 1 1 1 1 1 0]
Polynomial_2	$X^{13}+X^{4}+X^{3}+X+1$
Initial State_2	[1 1 1 1 1 1 1 1 1 1 1 1 1]

TABLE 3. Code generator polynomials and initial states for generating the first 8,190 bits of the Compass E6 I-channel signal

E6 I-channel code (Tail)	
Polynomial_1	$X^{13}+X^{12}+X^{10}+X^{9}+X^{7}+X^{6}+X^{5}+X+1$
Initial State_1	[1 1 1 1 1 1 1 1 1 1 1 1 1]
Polynomial_2	$X^{13}+X^{4}+X^{3}+X+1$
Initial State_2	[1 1 1 1 1 1 1 1 1 1 1 1 1]

TABLE 4. Code generator polynomials and initial states for generating bits 8,191-10,230 (last 2,040 bits) of the Compass E6 I-channel signal

Compass Broadcast		Type	Primary Code Period	Code Generators	Secondary Code Period	Data
E2	I-channel	BPSK(2)	1 ms	11-stage Gold code	20 ms	Yes
E5b	I-channel	BPSK(2)	1 ms	11-stage Gold code	20 ms	Yes
E6	I-channel	BPSK(10)	1 ms	Two 13-stage Gold code	20 ms	Yes

TABLE 5. Summary of Compass M-1 Broadcast Code Results (I-Channel only)

This latter phenomenon is caused by the acquisition algorithm estimating the code phase to the nearest sample, while — due to the choice of sampling rate — there are only two-and-a-half samples per chip. The result is that our estimate may be off by as much as a quarter of a chip. The data shown in Figure 11 confirms this, as our estimate is never greater than ¼ chip (~40 m) during convergence. The Doppler frequency is locked at 700 Hz, as shown in the lower-left plot in Figure 11.

Summary of Compass M-1 Codes

The E2 signal also has a component in quadrature. Analysis of this component indicates a much longer sequence (> 100 milliseconds) than the inphase BPSK(2) code described previously. In fact, the Q-channel codes on all frequencies (E2, E5b, E6) appear to share this characteristic. At present, we are still processing data to assess its characteristics and to determine the Q-channel code length.

Two signals occupy the E5 band: a BPSK(2) and a BPSK(10). Many observers have noted that the E2 I-channel and E5b BPSK(2) codes are identical. This has been verified through acquisition and tracking of E5b I-channel using the E2-derived I-channel code.

The E6 signal uses QPSK(10) modulation. The Compass E6 I-channel primary code is one millisecond long and has 10,230 bits. Unlike the Galileo or the Compass E2 primary codes, the Compass E6 I-channel code is composed of segments from two codes.

We designated these two codes as E6_head and E6_tail. E6_head provides the first 8,190 bits of the code sequence. E6_tail contains the 8,191st bit to the 10,230th bit in the sequence. Both E6_head and E6_tail are 13-stage Gold codes with the identical code generator polynomials. The only difference between them is the initial states of the code generator polynomial.

The code generators and initial conditions for the E6_head and E6_tail sequence are presented in Table 3 and Table 4, respectively. Furthermore, the E6 I-channel also has a 20-bit Neuman-Hoffman secondary code sequence that is identical to the one used in E2 (and E5b). The secondary code has 20 bits as follows:

E6 I-Channel Secondary Code: -1 -1 -1 -1 -1 1 -1 -1 1 1 -1 1 -1 1 -1 -1 1 1 1 -1

Table 5 provides a summary of the codes that we have currently determined. As more data is processed and we ascertain additional results, they will be posted on our website at <waas.stanford.edu>.

Manufacturers

Stanford University researchers use an Agilent 89600 vector signal analyzer from **Agilent Technologies**, Palo Alto, California, USA, to collect signals received at the SGMS. The skyplot in Figure 1 was generated with satellite tracking software, Nova for Windows, developed by **Northern Lights Software Associates,** Jamesville, New York USA.

References

[1] Bian, S., and J. Jin, and Z. Fang, "The Beidou Satellite Positioning System and Its Positioning Accuracy," *Navigation: The Journal of the Institute of Navigation*, Vol 52, Number 3, Fall 2005.

[2] "China to Build Global Satellite Navigation System," The People's Daily Online, 16 April 16, 2007 <http://english.people.com.cn/200704/16/eng20070416_366845.html>

[3] "China Announces Plans for Its Own GNSS," *Institute of Navigation Newsletter*, Vol. 16. Num. 3 (Fall 2006) <http://www.ion.org/newsletter/v16n3.pdf>

[4] Grelier, T., and J. Dantepal, A. Delatour, A. Ghion, and L. Ries, "Initial Observations and Analysis of Compass MEO Satellite Signal," Inside GNSS, May/June 2007

[5] Gao, G. X., and J. Spilker, T. Walter, P. Enge and A. R. Pratt, "Code Generation Scheme and Property Analysis of Broadcast Galileo L1 and E6 Signals", ION GNSS 2006, Fort Worth, Texas, USA, September 2006

[6] Gao, G. X., and D. De Lorenzo, A. Chen, S. Lo, D. Akos, T. Walter, and P. Enge, "Galileo Broadcast E5 Codes and Their Application to Acquisition and Tracking", Institute of Navigation National Technical Meeting, San Diego, California, USA, January 2007

[7] Lo, S. and A. Chen, P. Enge, G. Gao, D. Akos, J.-L. Isssler, L. Ries, T. Grelier, and J. Dantepal, "GNSS Album : Images and Spectral Signatures of the New GNSS Signals," Inside GNSS, May/June 2006

[8] Spilker, J., *Digital Communications by Satellite*, Prentice-Hall Information Theory Series, 1977

Authors

Alan Chen is a Ph.D. candidate in the Department of Aeronautics and Astronautics at Stanford University. He received an M.S. from that department and received his S.B. degree in aeronautics and astronautics from MIT. His current research interest involves unexploded ordnance, sensor fusions, autonomous helicopter, and GNSS signals.

David De Lorenzo is a research associate at the Stanford University GPS Research Laboratory. He received the Ph.D. in aeronautics and astronautics from Stanford University with thesis research on adaptive antenna arrays, their ability to reject radio frequency interference, and their impact on GPS measurement errors. He has previously worked for Lockheed Martin and for the Intel Corporation.

Per Enge is a professor of aeronautics and astronautics at Stanford University, where he is the Kleiner-Perkins, Mayfield, Sequoia Capital Professor in the School of Engineering. He directs the GPS Research Laboratory, which develops satellite navigation systems based on the Global Positioning System (GPS). He has been involved in the development of Federal Aviation Administration's GPS Wide Area Augmentation System (WAAS) and Local Area Augmentation System (LAAS) for the FAA. Enge has received the Kepler, Thurlow, and Burka Awards from the Institute of Navigation. He received his Ph.D. from the University of Illinois.

Grace Xingxin Gao is an Electrical Engineering Ph.D. candidate in the GPS Laboratory at Stanford University. She received a B.S. in mechanical engineering and her M.S. in electrical engineering from Tsinghua University, Beijing, China. Her current research interests include Galileo signal and code structures, GNSS receiver architectures, and GPS modernization.

Sherman Lo is a research associate at the Stanford University GPS Research Laboratory managing the assessment of Loran for civil aviation and also works on a variety of GNSS-related issues. He received his Ph.D. in aeronautic and astronautics from Stanford University. He has received the Institute of Navigation (ION) Early Achievement Award and the International Loran Association (ILA) President's Award.

IG